Mobicast Routing Protocol for Underwater Sensor Networks

Yuh-Shyan Chen and Yun-Wei Lin

***Abstract*—In this paper, we investigate a mobicast, also called a mobile geocast, problem in three-dimensional (3-D) underwater sensor networks (USNs), which aims to overcome the hole problem and minimizes the energy consumption of the sensor nodes while maximizing the data collection. In this paper, all underwater sensor nodes are randomly distributed in a 3-D underwater environment in the sea to form a 3-D USN. Considered a mobile sink or an autonomous underwater vehicle (AUV), all possible sensor nodes near the AUV form a 3-D geographic zone called a 3-D zone of reference (3-D ZOR). The AUV travels a user-defined route and continuously collects data from sensor nodes within a series of 3-D ZORs at different times. The main problem is how to efficiently collect data from sensor nodes within a 3-D ZOR while those sensor nodes are usually in sleep mode for a long period. The routing protocol relies on two phases: the first phase consists of collecting data within a 3-D ZOR, and the second phase consists of waking up those sensor nodes in the next 3-D ZOR to be queried while trying to avoid topology holes. To save power, only sensor nodes in a 3-D ZOR are notified to enter the active mode in order to deliver sensed results to the AUV. The specific characteristics of USNs, including low communication bandwidth, large propagation delay, and ocean current, are significantly different from wireless sensor networks. To consider the characteristics of USNs, a new mobicast routing protocol is developed in 3-D USNs. The key design challenge is to develop a power-saving mobicast protocol in 3-D USNs to overcome the unpredictable 3-D hole problem. To solve the hole problem, an "apple slice" technique is used to build multiple segments to surround the hole and to assure routing path continuity. Finally, performance analysis is derived, and simulation results illustrate the performance improvement in successful delivery rate, power consumption, and message overhead.**

***Index Terms*—Geocast, mobicast, multicast, routing, underwater sensor network.**

I. Introduction

UNDERWATER sensor networks (USNs) consist of number of *underwater sensor nodes* or just called *sensor* nodes which are equipped with acoustic transceivers that enable them to communicate with each other to perform collaborative sensing tasks over a given area [1] from shallow water and seabed. USNs have many potential applications in ocean monitoring, such as current flow, oil pollution, seismic and tsunamis monitoring, to supply the high spatiotemporal resolution capability. Sensor nodes report the sensed data to a control station on the ocean surface for investigation.

The power consumption issue are mainly focused on USNs [2], because that the battery power of a sensor node is a valuable resource and it is very difficult to recharge in the sea. Acoustic communications in the ocean is feasible for the data transmission; unfortunately, the propagation delay is comparatively large, compared to the low propagation delay of radio wave used in the air. An ocean current is a continuous, directed movement of ocean water generated by the forces acting upon the mean flow. Underwater sensor nodes always be drifted caused by the ocean current, the location of sensor nodes in the ocean is usually changed caused by the ocean current. The USN is thus with the changeable topology over time. In addition, the network fragmentation or hole problem is occurred because that there is no uniform distribution of underwater sensor nodes and the ocean current.

In USNs, one way to collect the sensed data from all underwater sensor nodes is directly transmitting the sensed data to the control station on the ocean surface. It takes a long route path [3] between sensor nodes with the control station on the ocean surface. It is observed that the control station always collects the inaccurate sensed data since the long route path has the higher probability of encountering the hole problem. One easy way to reduce the probability of encountering the hole problem and improve the accurate sensed data is to use the AUV (autonomous underwater vehicle) [4]. The AUV is a mobile sink and designed to nearly collect the sensed data from sensor nodes and indirectly report to the control station with the short route path. The AUV usually travels a circle path around a given observed area. The AUV collects the sensed data along the travelled circle path, and finally reports the aggregative sensed data to the control station when the AUV is approaching to the control station; even so, AUV still encounters the hole problem and the ocean current effect.

A new multicast communication paradigm called a "spatiotemporal multicast" or "mobicast" was recently investigated [5], [6] in wireless sensor networks (WSNs). The distinctive feature of mobicast is the delivery of information to all nodes that happen to be in a prescribed region of space at a particular point in time. Mobicast considers both spatial and temporal factors for delivering data, which is suitable for an AUV to collect the sensed data in the sea. However, USNs are fundamentally different to WSNs. It is known that USNs

Manuscript received December 15, 2011; revised June 27, 2012; accepted October 19, 2012. Date of publication November 12, 2012; date of current version January 14, 2013. This work was supported by the National Science Council of China under Grant NSC-98-2221-E-305-003 and Grant NSC-100-2221-E-305-001-MY3. The associate editor coordinating the review of this paper and approving it for publication was Prof. Elliott R. Brown.

The authors are with the Department of Computer Science and Information Engineering, National Taipei University, Taipei, Taiwan (e-mail: yschen@mail.ntpu.edu.tw; jyneda@gmail.com).

Color versions of one or more of the figures in this paper are available online at http://ieeexplore.ieee.org.

Digital Object Identifier 10.1109/JSEN.2012.2226877

consist of a set of floating sensor nodes and WSNs consist of a set of static sensor nodes. The topology of WSNs is stable, but the topology of USNs is changeable caused by the ocean current. The propagation delay in USNs is much longer than in WSNs when sensor nodes communicate to each other. WSNs are usually deployed on a two-dimensional plane, which are different from USNs. USNs are deployed in a three-dimensional space. Those key differences lead to existing mobicast protocols in WSNs can not be directly applied to USNs. Consequently, efforts will be made in this paper to develop a new mobicast protocol for three-dimensional USNs.

In this paper, a geographic zone, called as 3-D zone of relevance (3-D ZOR), is prescribed by an AUV to collect sensed data from all sensor nodes located in 3-D ZOR. The spatiotemporal character of a mobicast is to collect the sensed data from sensor nodes that will be present at time t in the 3-D ZOR, where both the location and shape of the 3-D ZOR are a function of time over some interval (t_{start}, t_{end}). Assumed that an AUV travels a circle path around a given observed area. The AUV constructs a series of 3-D ZORs over different intervals (t_{start}, t_{end}), and only sensor nodes located in the 3-D ZOR at the time interval (t_{start}, t_{end}) must wake up to send sensed data to the AUV. It is observed that 3-D ZOR is evolved and continuously moves with the AUV over time.

To save power and send sensed data to the AUV, sensor nodes in 3-D ZOR must be waken up and keep the active mode to wait for the arrival of AUV. The AUV cannot successfully receive the sensed data in time if sensor nodes in 3-D ZOR are still in the sleep mode. This problem is more seriously in USNs because that propagation delay of USNs is larger than that of WSNs. A good mobicast routing protocol in USNs must notifies the sensor nodes in 3-D ZOR at time t in time, even if there is hole problem and the ocean current effect.

The specific characteristics of USNs, such as low communication bandwidth, large propagation delay, and ocean current are significantly different from wireless sensor networks (WSNs). To consider the characteristics of USNs, a new mobicast routing protocol is developed in 3-D USNs. This is the first result to develop a mobile geocast routing protocol in USNs. The key design challenge is to develop a power-saving mobicast protocol in 3-D USNs to overcome the unpredictable 3-D hole problem. A "apple peel" scheme of the mobicast protocol is proposed to solve the unpredictable 3-D hole problem. Finally, performance analysis is derived and simulation results illustrate the performance improvement in successful delivery rate, power consumption, and message overhead.

The rest of this paper is organized as follows. Section II reviews related works. Section III presents the challenges and basic ideas. Section IV presents the new mobicast routing protocol. Performance analysis is discussed in Section V. Finally, Section VI concludes this paper.

II. Related Works

Collecting sensed data from sensor nodes with the requirement of power saving should take both spatial and temporal issues into consideration. Only sensor nodes closed to a mobile sink should participate in the data collection, and the other sensor nodes stay at sleep mode for the power saving. This task can be facilitated by a spatiotemporal multicast protocol which called "mobicast." Mobicast can consider both spatial and temporal issues to provide a spatiotemporal solution for the data collection and dissemination. The design of mobicast is to provide a spatiotemporal solution to deliver messages to the right place at the right time. Protocols for supporting mobicast is not yet investigated in USNs, but similar problems [5], [6] had been investigated in WSNs. A spatiotemporal multicast protocol, namely a mobicast, was presented in WSNs [5], [6]. The spatiotemporal characteristic of a mobicast is to forward a message to all nodes that will be present at time t in the forwarding zone [5], [6]. Chen *et al.* [5], [6] proposed a variant-egg (VE)-based mobicast routing protocol in sensornets.

However, all existing mobicast routing strategies are applied to WSNs. It is observed that a USN is natively different from a WSN. A USN consists of many floating sensor nodes in a 3-D space, while WSN consists of many static sensor nodes in a 2-D plane [5], [6]. The topology of a WSN is always stable, but topology of a USN is changeable because sensor nodes can be drifted by ocean currents. This causes the *link disconnection* problem or *hole* problem in USNs. With the hole problem, mobicast messages may not be successfully delivered. This is because that the USN is incurred the effect of ocean currents, but this problem never be occurred in the WSN. In addition, the impact of a long propagation delay on the data transmission in a 3-D underwater environment must be further considered when designing the 3-D routing protocols [7].

Sanjay *et al.* [8] proposed a 2-D geocast routing protocol with hole detection in USNs to provide the data dissemination in a target region. The source node delivers the data to a target region using a greedy forwarding technique. When the data delivers into the target region, the first node which receives the data serves as a root to construct a multicast tree for data delivery within the target region. The data is only disseminated in the target region. If a node cannot further deliver the data and does not reach the boundary of the target region, the node detects a hole. A virtual area is used to expand the target region to involve more nodes for data delivery to overcome the hole. This protocol provides a data dissemination technique with a high successful rate for a static region in 2-D USNs. However, sensor nodes usually deploy in a 3-D environment in most of USNs. The routing path, the target region and the hole in a 3-D USNs are variform, which needs to be further investigated.

To achieve the purpose of the reliable data collection, an AUV is usually used to effectively collect the sensed data from sensor nodes [4], [9], [10]. Walker [4] proposed an exploring solution in the underwater environment. A traveling AUV roams around in a USN and collects sensed data from those sensor nodes, and then the AUV uploads collected data to a base station. Walker shows the AUV is feasible and useful to distributed collect data in the underwater environment. Wang *et al.* [9] proposed a solution to collect data with multiple AUVs. Wang *et al.* well divide a large USN into several sub-regions and assign an AUV in each sub-region to collect data. Multiple AUVs simultaneously collect data in different sub-regions and upload collected data to a base station. The end-to-end delay and energy cost can be reduced because the data is parallel collecting and the routing path in each sub-region is short. Seah *et al.* [10] proposed a multiple AUVs approach to overcome the network fragmentation problem for improving the network connectivity. The network fragmentation could be happened since sensor nodes are non-uniform distribution and can be drifted away by ocean currents. Multiple AUVs search for and identify critical communication gaps between network fragmentations among a USN, and if a AUV finds a critical communication gap, the AUV acts as a bridge between two network fragmentations and enhances the connectivity of the network. Therefore, AUVs can be useful and reliable to collect sensed data from sensor nodes. The above-mentioned AUV results [4], [9], [10] focus on how to improve the data collection efficiency of AUVs. However, those protocols do not consider to collect data from sensor nodes which may stay at sleep mode. Sensor nodes usually stay at sleeping mode for power saving. A sensor node cannot be immediately waked up by a waking up message sent from an AUV when the AUV is closing to the sensor node because the waking up message should propagate with a long delay in the sea. Besides, the waking up message may fail to deliver and does not wake up sensor nodes because the link connectivity is lost due to the hole problem and the ocean current effect. The AUV fails to collect sensed data from a sensor node if the sensor node stays at sleep mode. This is, to achieve a successful data collection, an AUV should wake up sensor nodes in advance to prepare for data transmission while an AUV is approaching. In this paper, a 3-D prescribed region which the AUV is going to collect data denotes as a 3-D ZOR. To assist an AUV in successfully collecting sensed data from sensor nodes, this paper proposes a distributed mobicast routing protocol to deliver mobicast messages for waking up all sensor nodes in a 3-D ZOR at time t. To our knowledge, this work is the first study to develop the mobicast routing protocol in USNs.

III. Preliminaries

This section presents the system model and basic idea. The contribution and the application examples are also introduced.

A. System Model

In this work, sensor nodes are randomly deployed in the ocean. Sensor nodes may be drifted by ocean currents. We assume each sensor node can know its location by range-based or range-free localization techniques [11]. Fig. 1 shows the architecture in this work. The AUV travels along a user-defined route with a constant velocity and collects sensed data from sensor nodes in a series of 3-D ZORs. The AUV should accomplish the route before the user-defined response time, and then the AUV returns to report the collected data to a control station. Each sensor node can record its locations at each time stamps to calculate the drifted speed. When a sensor node detects the drifted speed, that means there exists an ocean current at the present position and the speed of the ocean current is the drifted speed of the sensor node. The speed of AUV is depended on the user-defined response time. Based on the distance of user-defined path and response time, the AUV can calculate a proper speed using the distance divided by response time. When the AUV encounters an ocean current, the AUV should be accelerated or decelerated to compensate for the effect of the ocean current. Sensor nodes usually stay at sleep mode for power saving. If the AUV wants to successfully collect sensed data, sensor nodes should stay at active mode. Since the AUV should accomplish the route before the user-defined response time, the AUV cannot stop to wait for a sensor node to switch to active mode. Moreover, considering the ocean current, a pre-defined waking up schedule is not suitable for data collection since sensor nodes are drifted to different location at different time. Also, sensor nodes cannot wake up immediately due to the long propagation delay when the AUV is arrivered. Hense, sensor nodes should be waked up first while the AUV is approaching. This is, sensor nodes located at right "place" and at right "time" should be waked up to send sensed data. The right "place" means the 3-D ZOR which the AUV arrives. The right "time" means the time while the AUV is approaching. This wake up procedure is controlled by the mobicast protocol. It is inappropriate to use a long range transmission for a wake up notification due to

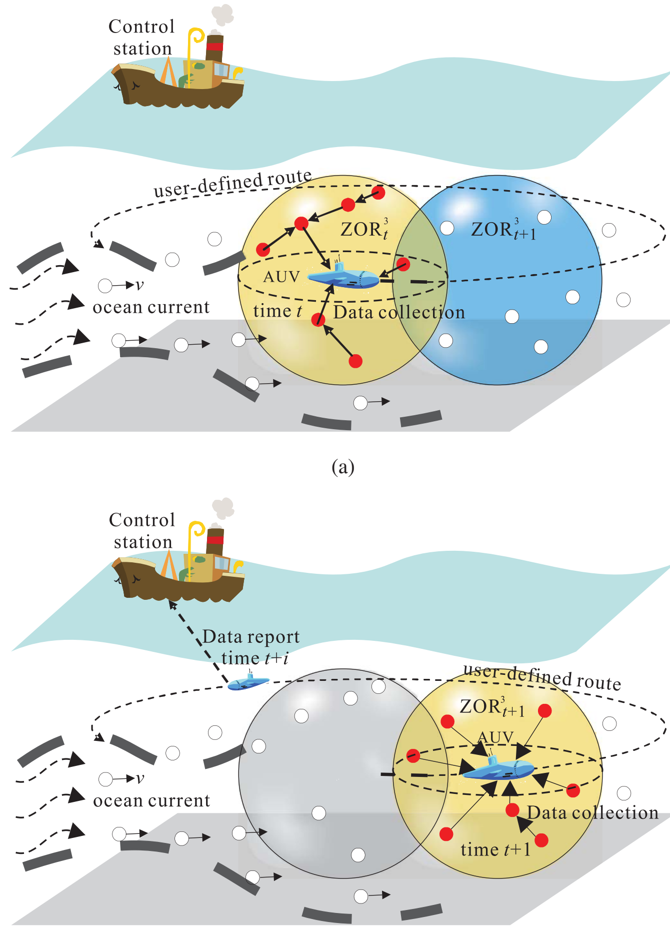

(a)

(b)

Fig. 1. AUV collects data form sensor nodes in (a) ZOR$_t^3$ at time t and (b) ZOR$_{t+1}^3$ at time $t+1$.

the long propagation delay time since the condition of sensor nodes may be different. A short range transmission should be used for the wake up notification; therefore, the wake up notification is sent by the AUV to sensor nodes when the AUV is close to sensor nodes with a short distance. The correct sensor nodes can be waked up precisely at a correct position and a correct time. Besides, If the wake up schedule is announced using a simple broadcast protocol by the control station, sensor nodes located at the AUV's travel path cannot be waked up precisely at a correct position and a correct time due to the long propagation delay time and the ocean current. Sensor nodes located at the AUV's travel path are different at different time because sensor nodes may be drifted away by the ocean current. If the wake up schedule is previously broadcasted from control station, the AUV may meet the other sensor nodes which do not receive the wake up schedule, then the AUV is failed to collect data from there sensor nodes at sleep mode. Therefore, the only way to ensure sensor nodes located at the AUV's travel path can be correctly waked up, the wake up schedule should be sent by the AUV when the AUV is approaching to these sensor nodes.

The mobicast protocol is to forward a mobicast message to wake up all sensor nodes that will be present at time t in a 3-D ZOR. However, the mobicast message may not be successfully delivered to wake up all sensor nodes within the 3-D ZOR due to the hole problem. A partial sensor nodes may still stays at sleep mode. That causes the AUV fails to collect sensed data from those sensor nodes at sleep mode. To overcome the hole problem and wake up all sensor nodes in the 3-D ZOR, a 3-D geographic zone (called the 3-D zone of forwarding, 3-D ZOF) is prescribed by the AUV. The 3-D ZOF is comprised of sensor nodes which will be present at time $t+1$ in the 3-D ZOF, which is responsible for forwarding the mobicast messages in order to guarantee that sensor nodes in the 3-D ZOR at time $t+1$ can successfully wake up. The size of ZOF is always larger than or equal to the size of ZOR.

In the following, we define 3-D ZOR_t (3-D zone of relevance) and 3-D ZOF_{t+1} (3-D zone of forwarding). Let N_i denote as the ID of a sensor node, where $i = \{1, 2, \ldots, i, i+1, \ldots, n\}$ throughout this paper. The 3-D ZOR_t is a geographic zone created by the AUV at time t to indicate which sensor node should send the sensed data to the AUV. The AUV can collect sensor data from all sensor nodes in the USN by creating a series of 3-D ZOR_t at different time t. A formal definition of 3-D ZOR_t is given.

Definition 1 3-D ZOR_t or ZOR_t^3 (3-D Zone of Relevance): Given an AUV, 3-D ZOR_t is a 3-D spherical region determined by AUV at time t, such that sensor node N_i must transmit the sensed data to AUV at time t, where N_i is located in the 3-D ZOR_t. The center location of 3-D ZOR_t is the same with the location of AUV, moving at the same speed as AUV, and toward the same direction with AUV.

Fig. 1 shows an example of 3-D ZOR_t^3, where the time is from t to $t+1$. The AUV collects sensed data from sensor nodes located in ZOR_t^3 at time t. To continuously collect sensed data from all sensor nodes in the USN, a new ZOR_{t+1}^3 should be created for data collection at time $t+1$. Sensor nodes usually stay at sleep mode for power saving. To wake

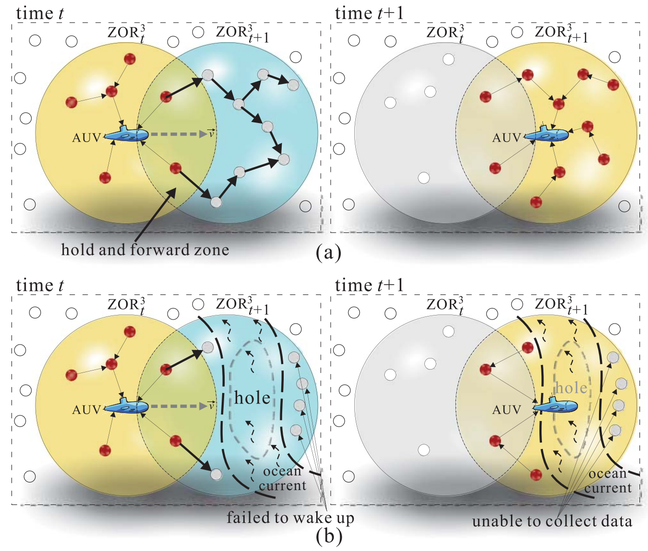

Fig. 2. (a) Successful data collection. (b) AUV failed to collect data from part sensor nodes due to ocean current.

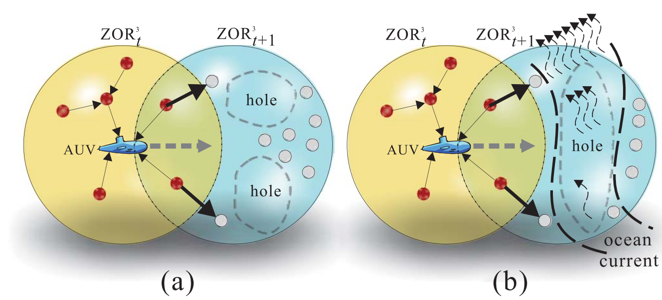

Fig. 3. Hole problem is occurred due to (a) nonuniform distribution and (b) ocean current.

up those sensor nodes within ZOR_{t+1} in advance, a "hold and forward" zone is used. The hold and forward zone is an overlapping area between ZOR_t^3 and ZOR_{t+1}^3 as shown in Fig. 2(a). Sensor nodes located in the hold and forward zone should wake up all sensor nodes in ZOR_{t+1}^3 by delivering the mobicast message. Then the AUV can collect sensed data from sensor nodes in ZOR_{t+1}^3 at time $t+1$. However, sensor nodes may be drifted away by ocean current and that causes the hole problem. The mobicast message cannot not be delivered to some sensor nodes within ZOR_{t+1}^3 because the hole problem causes a feasible routing path to some sensor nodes within ZOR_{t+1}^3 may not exist. Some sensor nodes can not be waked up to prepare for sending data. Fig. 2(b) shows an example of mobicast with the hole problem. At time $t+1$, a partial sensor nodes in ZOR_{t+1} are failed to be waked up due to the hole problem. Fig. 3(a) shows the hole problem is occurred due to non-uniform distribution of sensor nodes; moreover, the ocean current can aggravate the hole problem. Fig. 3(b) shows the variant speed of an ocean current can change the distribution of sensor nodes. Sensor nodes easily gather in an area with a slower speed current than an area with a higher speed current. Fig. 4 shows that sensor nodes are gathering when the ocean current changes to slower speed and sensor nodes do not stay when the ocean current changes to higher speed. That causes

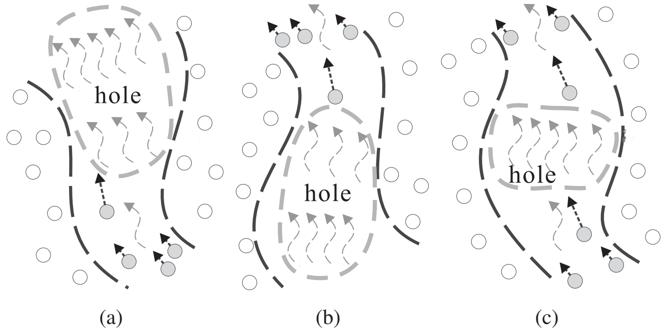

Fig. 4. Sensor nodes are nonuniform distribution due to the changeable velocity of ocean currents. (a) and (b) Sensor nodes are drifted by ocean currents. (c) Sensor nodes are separated by ocean currents.

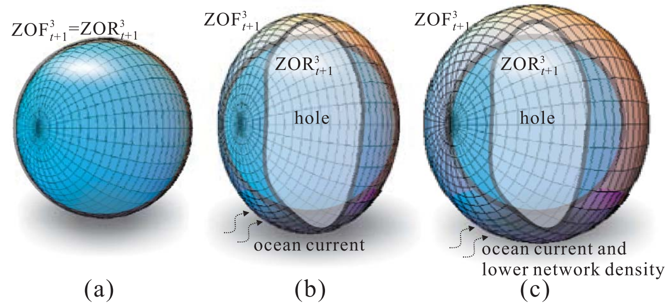

Fig. 6. ZOF^3_{t+1} expands to cover the hole based on the network density and the ocean current. (a) No hole. (b) Hole with ocean current. (c) Hole with ocean current and low network density.

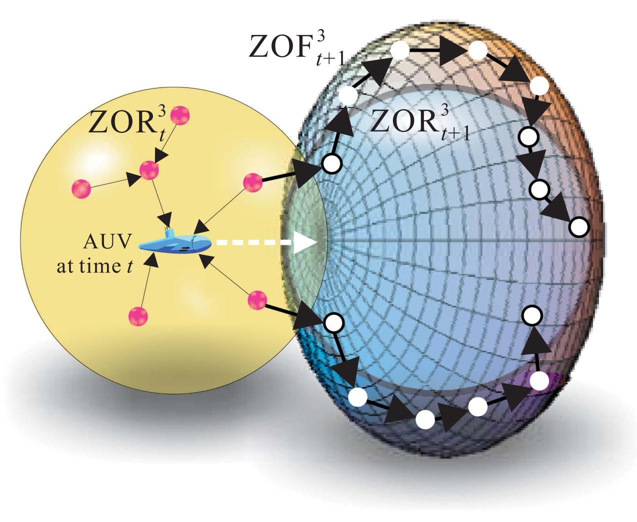

Fig. 5. ZOF^3_{t+1} is oblate spheroidal region and covers ZOR^3_{t+1}.

the more serious hole problem. To overcome the hole problem, a zone of forwarding 3-D ZOF_{t+1} is created by the AUV at time t. The 3-D ZOF_{t+1} is a geographic zone created by the AUV at time t to indicate which sensor node should deliver the mobicast message for waking up sensor nodes within ZOR^3_{t+1}. A formal definition of 3-D ZOF_{t+1} is given.

Definition 2 3-D ZOF_{t+1} or ZOF^3_{t+1} (3-D Zone of Forwarding): Given an AUV, 3-D ZOF_{t+1} is a 3-D oblate spheroidal region determined by AUV at time t, such that each sensor node N_i in the 3-D ZOF_{t+1} has the responsibility of forwarding the mobicast message to sensor nodes within 3-D ZOR_{t+1}.

Fig. 5 shows an example of 3-D ZOF_{t+1}. ZOF^3_{t+1} is always larger than ZOR^3_{t+1} and covers ZOR^3_{t+1}. Although a feasible routing path does not exist in ZOR^3_{t+1} due to the hole problem, an alternative routing path can be discovered in ZOF^3_{t+1} to deliver the the mobicast message. The hole problem is solved.

However, since the battery power in USNs is a valuable resource, sensor nodes within ZOF^3_{t+1} should be carefully chosen for the mobicast message delivery. In a 3-D ZOF_{t+1}, there are multiple routing paths which can be used to deliver the mobicast message. With the consideration of the direction of current flow, the successful delivery rate is different on different routing paths. We discuss how to select routing paths to achieve the highest successful delivery rate and save power in the next section.

B. Basic Idea

Our mobicast protocol enables the AUV to collect sensed data in from those sensor nodes which usually stay at sleep mode for power saving in the 3-D USN; meanwhile, the hole problem and the ocean current effect are also considered. To successfully collect sensed data, the AUV delivers a mobicast message at time t to wake up all sensor nodes which will be present at time $t+1$ within ZOR^3_{t+1}. To overcome the hole problem and wake up all sensor nodes within ZOR^3_{t+1}, ZOF^3_{t+1} is used to cover the potential 3-D hole and discover the routing paths for the mobicast message delivery. To ensure that sensor nodes within ZOR^3_{t+1} can be waked up, two steps are used. The first step is to determine the size of ZOF^3_{t+1}, and the second step is to determine how many sensor nodes within ZOF^3_{t+1} are used to deliver the mobicast message.

The first step determines the size of ZOF^3_{t+1}. A large size of ZOF^3_{t+1} can overcome the hole problem and achieve higher successful delivery rate but consumes much power. On the other hand, a small size ZOF^3_{t+1} may not cover the hole and fail to wake up sensor nodes within ZOR^3_{t+1}. Therefore, the size of ZOF^3_{t+1} should be carefully considered. To overcome the 3-D hole in ZOR^3_{t+1}, the drifted distance of sensor nodes is the major concern. ZOF^3_{t+1} should be capable of covering a sensor node even if the sensor node is drifted by ocean currents. Therefore, the size of ZOF^3_{t+1} is determined by the velocity of ocean currents and the network density. If there is no ocean current within ZOR^3_t, the size of ZOF^3_{t+1} is equal to the size of ZOR^3_{t+1}, as shown in Fig. 6(a). If there exists an ocean current within ZOR^3_t, the size of ZOF^3_{t+1} is enlarged based on the velocity and direction of the ocean current to cover the drifted sensor nodes as shown in Fig. 6(b). This is because that sensor nodes are drifted away by the ocean current and then the hole may be enlarged. Therefore, ZOF^3_{t+1} should be also enlarged to cover the potential hole. If the network density is getting lower in ZOR^3_t, ZOF^3_{t+1} is expanded to a larger size to cover more sensor nodes for route discovery, as shown in Fig. 6(c). Observe that, it may be not accurate to predict the size of ZOF^3_{t+1} using the information in ZOR^3_t; therefore, a size adjustment scheme based on real-time information in ZOF^3_{t+1} is proposed to get the proper size of ZOF^3_{t+1}.

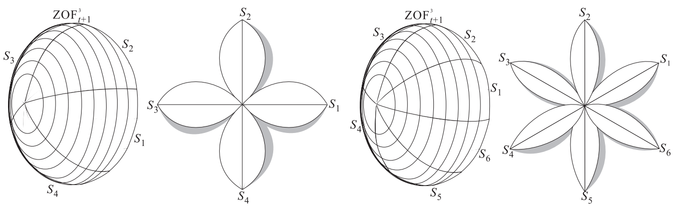

(a) (b)

Fig. 7. Oblate spheroidal of ZOF$^3_{t+1}$ is split into (a) four and (b) six segments.

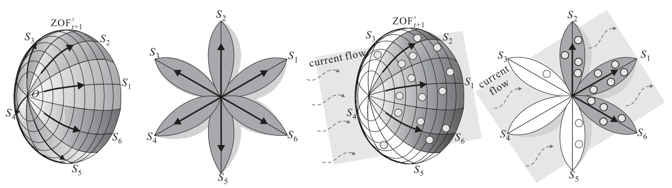

(a) (b)

Fig. 8. Messages delivery using (a) all segments and (b) only segments S_1, S_2, and S_6.

The second step determines how many sensor nodes are used to deliver the mobicast message. With the consideration of the ocean current, the successful delivery rate within different parts of ZOF$^3_{t+1}$ are different. Therefore, to keep a high successful delivery rate and save power, the only sensor nodes which are necessary to wake up are those nodes belonging to those parts of ZOF$^3_{t+1}$ with a high successful delivery rate. To divide a ZOF$^3_{t+1}$ into several parts, we use a simple concept–slice apple, as shown in Fig. 7. We slice a ZOF$^3_{t+1}$ into m several identical parts. We called each part as a *segment*.

Definition 3 S_i (Segment): Given a 3-D oblate spherical ZOF$^3_{t+1}$, the geographic location of sensor nodes in the oblate sphere can be indicated as area "S." The area S can be divided into m identical parts. We called the each part of S as a segment S_i, where $i = 1, 2, \ldots, m$.

Fig. 7(a) and (b) show that ZOF$^3_{t+1}$ is split into four segments and six segments, respectively. The key idea of this work is to use those sensor nodes in those segments to deliver the mobicast for waking up sensor nodes in ZOR$^3_{t+1}$.

The mobicast message is delivered by those sensor nodes as could as possible. Fig. 8(a) shows that the mobicast message is successfully delivered within all segments without ocean currents. Fig. 8(b) illustrates that the mobicast message is delivered within only S_1, S_2, and S_6 when there is the ocean current. Sensor nodes are drifted out some segments by the ocean current and that causes the unsuccessful message delivery. To overcome the ocean current effect, the size of a segment can adaptively expand based on the real-time velocity and direction of the ocean current in ZOF$^3_{t+1}$. Fig. 9(a) shows the size of segment S_1 is small if the velocity of the ocean current in ZOF$^3_{t+1}$ is slow and Fig. 9(b) shows the size of segment S_1 is large if the velocity of the ocean current in ZOF$^3_{t+1}$ is fast. When the size of a segment is expanded, more sensor nodes are used to deliver the mobicast message and the successful delivery rate is improved. The detailed algorithm of the mobicast routing protocol is given in the next section.

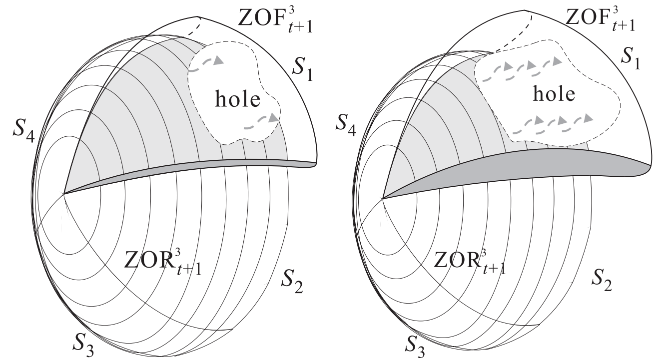

(a) (b)

Fig. 9. The segment adaptively expands to cover the hole. (a) Small hole. (b) Bigger hole.

C. Contribution

In this paper, a 3-D zone of forwarding is proposed to overcome the hole problem and the effect of ocean currents in order to forward the mobicast message to all sensor nodes in ZOR^3_t. The contributions are summarized as follows: (1) our mobicast protocol builds a adaptive 3-D oblate spheroidal ZOF$^3_{t+1}$ to overcome the hole problem; (2) our mobicast protocol is a fully distributed algorithm which effectively reduces the power consumption and message overhead for constructing ZOF$^3_{t+1}$ and forwarding overhead; (3) our mobicast routing protocol offers high successful delivery rate to deliver the mobicast message. ZOF$^3_{t+1}$ can adaptively expand to a large size to cover the 3-D potential hole based on the ocean current and the network density as shown in Fig. 6. With the adaptively size of ZOF$^3_{t+1}$, routing paths can be discovered with higher possibility, and sensor nodes within ZOR$^3_{t+1}$ can be successfully waked up to prepare for data delivery.

D. Application Examples

USNs are used to collect environment information in the ocean. With the consideration of the property of USNs, to report sensed data to a control station on the surface through a long routing path may encounter several issues. It is a more reliable way to use an AUV with the mobicast protocol for data collection as shown in Fig. 10. An AUV can travel around the whole USN and collect sensed data from sensor nodes in a ZOR. Sensor nodes in the ZOR should transmit sensed data to the AUV via a short routing path while the AUV is approaching. Sensor nodes should stay at active mode for sending sensed data. On the other hand, sensor node should stay at sleep mode for power saving when they are idle. Our mobicast protocol can control the data collection process. Sensor nodes only wake up for sending data while the AUV is approaching; therefore, our mobicast protocol achieves both data collection and power saving.

IV. Mobicast Routing Protocol

In this section, we describe how an AUV collects sensed data from sensor nodes with our mobicast protocol. Our mobicast protocol is split into three phases, 3-D ZOR$_t$ initiation phase, 3-D ZOF$_{t+1}$ creation phase, and 3-D ZOR$_{t+1}$

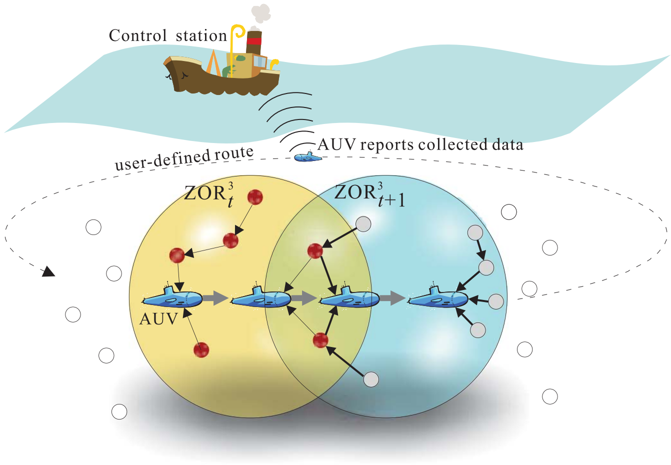

Fig. 10. AUV travels along a user-defined route and collects sensed data from sensor nodes in a 3-D ZOR.

collection phase. In 3-D ZOR_t creation phase, the AUV creates the ZOR_t^3 at time t to initiate the mobicast routing and delivers a mobicast message to wake up sensor nodes which will be present at time $t+1$ in ZOR_{t+1}^3. In 3-D ZOF_{t+1} creation phase, ZOF_{t+1}^3 is created with a proper size to cover the potential hole; meanwhile, ZOF_{t+1}^3 is split into several segments for the mobicast message delivery. In 3-D ZOR_{t+1} collection phase, the AUV collects the sensed data and from sensor nodes within ZOR_{t+1}^3. The detailed operation is developed as follows.

A. 3-D ZOR_t Initiation Phase

Sensor nodes located within ZOR_t^3 should send the sensed data to AUV. To collect sensor data from all sensor nodes in the USN, AUV should continuously create a series ZOR_t^3 at different time t. The procedure to create the ZOR_t^3 is given herein.

Step 1: AUV acquires the location (x_A, y_A, z_A) based on range-based or range-free localization techniques [11].

Step 2: To collect sensed data from sensor node, AUV creates the ZOR_t^3 by the equation $Z_t(N_i) = (x_i - x_A)^2 + (y_i - y_A)^2 + (z_i - z_A)^2 - R^2 = 0$, where R is the radius of ZOR_t^3, N_i is a single sensor node, (x_i, y_i, z_i) is the location of a sensor node N_i and (x_A, y_A, z_A) is the center of ZOR_t^3. $R = hop\_distance \times h$, where $hop\_distance$ is the communication range of a sensor node and h is a integer which is defined by a user to indicate a expected range for data collection. After AUV initiated the ZOR_t^3, ZOF_{t+1}^3 creation phase is executed.

Step 3: AUV broadcasts the mobicast control packet $P_m(N_i, Z_t(N_i), m, r, \overrightarrow{v_A})$, where P_m is the control packet to control the delivery of mobicast message, N_i is the ID of current sensor node, $Z_t(N_i)$ describes the region of ZOR_t^3, m is the mobicast message, r is the radius of hold and forward zone, and $\overrightarrow{v_A}$ is velocity vector of AUV. After AUV broadcasting the P_m, ZOF_{t+1}^3 creation phase is executed.

Step 4: A sensor node N_i should send the sensed data to the AUV if $Z_t(N_i) \le 0$ when a sensor N_i receives a P_m. $Z_t(N_i) \le 0$ implies sensor node N_i is located within ZOR_t.

Fig. 14 shows that a ZOR_t^3 with a R radius is created by $Z_t(N_i)$. Sensor nodes located within ZOR_t^3 should send sensed data to AUV at time t.

B. 3-D ZOF_{t+1} Creation Phase

To wake up sensor nodes located in the ZOR_{t+1}^3, ZOF_{t+1}^3 is necessary to create at time t. Sensor nodes within ZOF_{t+1}^3 should deliver the mobicast message to wake up those sensor nodes will be present within ZOR_{t+1}^3. To improve the successful delivery rate, ZOF_{t+1}^3 is divided into m identical segments and each segment can adaptively expand based on the network density and velocity of the ocean current to use more sensor nodes for mobicast message delivery. For this purpose, we should know how many total segments m should be sliced, and how many sensor nodes should be used to deliver the mobicast. To find the answers of above questions, we have lemmas below.

Lemma 1: Given a 3-D oblate spheroidal ZOF_{t+1}^3 and a vector of current flow $\overrightarrow{C}$; then we know the optimum segment quantity $m = \left\lceil \frac{2\pi a}{\overrightarrow{s_i^o} \cdot \overrightarrow{C}} \right\rceil$, where a is the equatorial radius of ZOF_{t+1}^3, $\overrightarrow{s_i^o}$ is an orthogonal vector of $\overrightarrow{s_i}$, where $\overrightarrow{s_i}$ is the message delivery direction in segment S_i.

Proof: A segment with a suitable size can achieve both high delivery rate and power saving. A segment with a larger size can tolerate a stronger current flow. This is because sensor nodes may not easily drift out of a large segment. A routing path could be easier to establish; therefore, the delivery rate is usually high in a segment with a large size. On the other hand, a segment with a large size involves more nodes to deliver messages and consumes much power. Hence, to find a suitable size of a segment is an important issue. A segment can tolerate a stronger current flow means that a sensor node does not drift out of the segment during the time interval $(t, t+1)$. Since the delivery direction is $\overrightarrow{s_i}$, $\overrightarrow{s_i^o}$ is the direction which a node drifts out of the segment. The distance which a node drifts during the time $(t, t+1)$ is $\overrightarrow{s_i^o} \cdot \overrightarrow{C} \times (t-t+1)$. $\overrightarrow{s_i^o} \cdot \overrightarrow{C}$ is the maximum velocity which a node drifts out of the segment. This is, if the width of a segment larger than $\overrightarrow{s_i^o} \cdot \overrightarrow{C} \times (t-t+1)$, then this segment can tolerate the current flow. Fig. 11 shows that a segment S_i has a arc length with $\overrightarrow{s_i^o} \cdot \overrightarrow{C} \times (t-t+1)$, and the total the arc length of a ZOF_{t+1} is $2\pi a$. This is, the surface of ZOF_{t+1} is divided into $m = \left\lceil \frac{2\pi a}{\overrightarrow{s_i^o} \cdot \overrightarrow{C}} \right\rceil$ identical segments; hence, the optimum segment quantity m is $\left\lceil \frac{2\pi a}{\overrightarrow{s_i^o} \cdot \overrightarrow{C}} \right\rceil$. ■

Fig. 11 shows the size of each segment is determined by the velocity of ocean current $\overrightarrow{C}$ and the delivery direction $\overrightarrow{s_i}$. A segment with a suitable size can tolerant the current flow. Fig. 12(a) shows that the size of segment is smaller when the velocity of current flow is slow. Fig. 12(b) shows that the size of segment is larger when the velocity of current flow is fast.

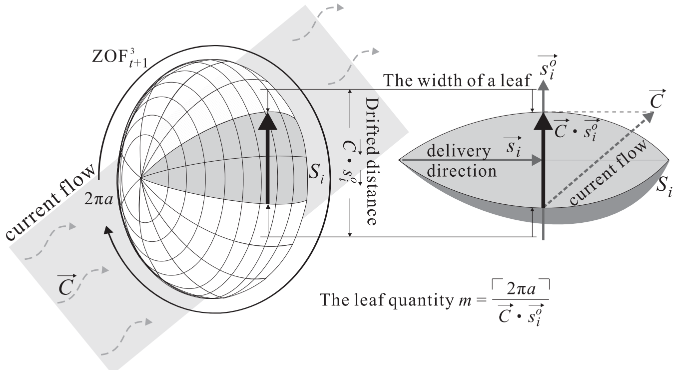

Fig. 11. Segment quantity m is decided according to the current flow.

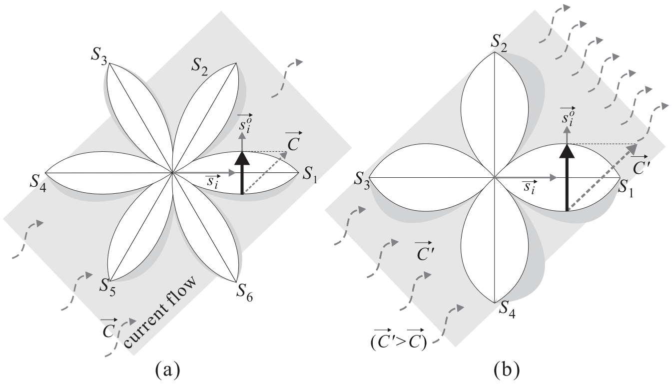

Fig. 12. The ocean current and the segment quantity. (a) Slow ocean current. (b) Strong ocean current.

Lemma 2: Assume that the successful communication rate of each sensor node is p. Given a successful prediction probability $(1-\alpha)$; then the minimum node quantity for getting the largest node efficiency is $n_m = (50\ Z_{\frac{\alpha}{2}}\sqrt{p(1-p)})^{\frac{2}{3}}$.

Proof: To find the minimum node quantity for getting the largest node efficiency, we should first know the failed delivery rate when how many sensor nodes are used to deliver a message. Let n denote as node quantity which means there are n sensor nodes to be involved for messages delivery. An error rate function $E(n) = \frac{Z_{\frac{\alpha}{2}}\sqrt{p(1-p)}}{\sqrt{n}}$ derived from Z-distribution [12] can be used to predict the failed delivery rate when there are n sensor nodes to be involved to deliver, where p is the successful communication probability when a node communicates with a neighboring node, $Z_{\frac{\alpha}{2}}$ is a z-value, and α is a probability which we fail to predict how many nodes are required. $Z_{\frac{\alpha}{2}}$ is a constant under the parameter α, which can find from a Z-distribution table. The error rate function $E(n)$ can help us to find the *node efficiency* with different node quantity. Let n_m denote the minimum node quantity for getting the largest node efficiency. Let ne denote as the node efficiency which represents how much error rate is reduced while one sensor node is added to deliver. The node efficiency $ne = 1$ implies each node can reduce 1% error rate. To efficiently deliver the mobicast message, the node efficiency ne should be large than or equal to 1. From the observation of error rate function $E(n)$, as shown in Fig. 13, we can know that the higher node quantity is, the lower error rate will be. Since the error rate drops as the node quantity increases, we

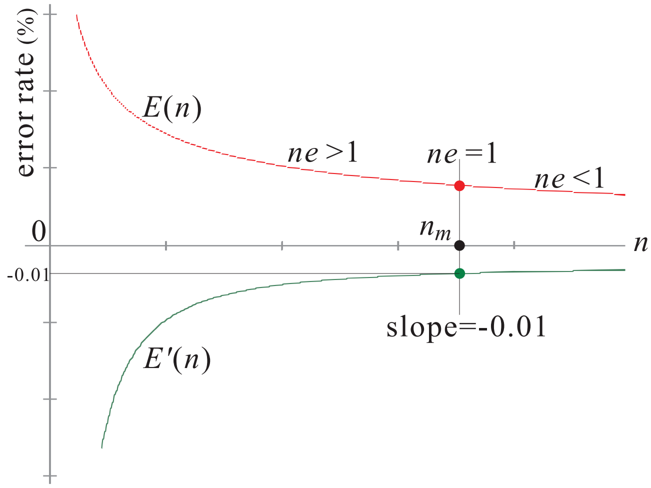

Fig. 13. Error rate versus the quantity of sensor nodes.

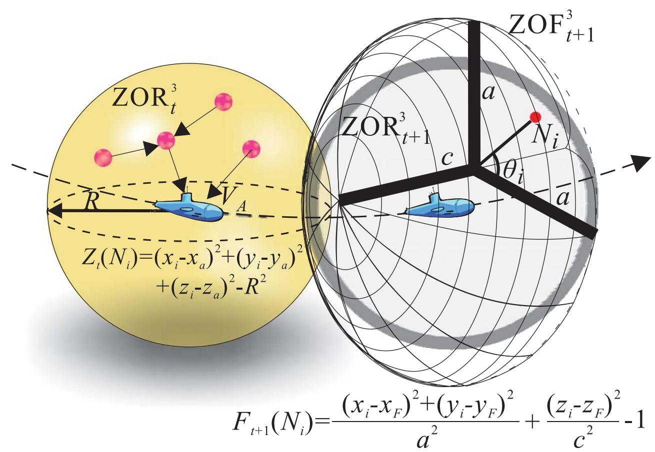

Fig. 14. Creation function of 3-D ZOR_t and 3-D ZOF_{t+1}.

can use the slope to describe the node efficiency ne. The slope means how much error rate can be reduced when one sensor node is added to deliver. Hence, the node efficiency ne is high when the slope is large. The first order differential of $E(n)$, $E'(n)$, describes the slope with different node quantity, where $E'(n) = -\frac{Z_{\frac{\alpha}{2}}\sqrt{p(1-p)}}{2}n^{-\frac{3}{2}}$. Therefore, $E'(n)$ can describe the node efficiency ne. The largest node efficiency with the minimum node quantity appears as $n = n_m$ when the slope is -0.01. This means each node can reduce 1% error rate when the node quantity is n_m. If the node quantity increases over n_m, each node can only reduce the error rate lower than 1%. That means the node efficiency $ne < 1$. To find n_m, we let $E'(n) = -0.01$. Then $n_m = (50\ Z_{\frac{\alpha}{2}}\sqrt{p(1-p)})^{\frac{2}{3}}$ is the minimum node quantity for getting the largest node efficiency. ■

The 3-D ZOF_{t+1} creation algorithm is presented as follows.

Step 1: To deliver the mobicast message for waking up sensor nodes in ZOR^3_{t+1}, ZOF^3_{t+1} is created by $F_{t+1}(N_i) = \frac{(x_i-x_F)^2+(y_i-y_F)^2}{a^2} + \frac{(z_i-z_F)}{c^2} - 1 = 0$, where (x_F, y_F, z_F) is the center of ZOF_{t+1}, a is the equatorial radius of ZOF^3_{t+1}, and c is the polar radius of ZOF^3_{t+1}. The size of ZOF^3_{t+1} is determined based on the network density and the current flow in ZOR_t^3. ZOF_{t+1}^3 should be able to tolerate the current flow and cover the hole; therefore, the size of ZOF_{t+1}^3 is expanded with the speed of the current flow. Let nd_t denote as the network density within ZOR_t^3, nd_{avg} denote as the average network density, and $\overrightarrow{C}$ denote as the velocity of current flow. The value of $a = R \times (1 + \frac{\overrightarrow{a} \cdot \overrightarrow{C}}{|\overrightarrow{C}|})$ and $c = R \times (1 + \frac{\overrightarrow{c} \cdot \overrightarrow{C}}{|\overrightarrow{C}|})$ if $nd_t \geq nd_{avg}$. Otherwise, $a = \frac{nd_{avg}}{nd_t} \times R \times (1 + \frac{\overrightarrow{a} \cdot \overrightarrow{C}}{|\overrightarrow{C}|})$ and $c = \frac{nd_{avg}}{nd_t} \times R \times (1 + \frac{\overrightarrow{c} \cdot \overrightarrow{C}}{|\overrightarrow{C}|})$ if $nd_t < nd_{avg}$. The condition $nd_t < nd_{avg}$ means that the network density is getting lower and ZOF_{t+1}^3 should expand to a larger size.

Step 2: To wake up sensor nodes in ZOR_{t+1}^3, sensor nodes located in a "hold and forward zone" should deliver the mobicast message through sensor nodes in ZOF_{t+1}^3. The hold and forward zone is a overlap between ZOR_t^3 and ZOR_{t+1}^3. The radius of the hold and forward zone is r, which is defined by a user.

Step 3: To achieve a high successful delivery rate, ZOF_{t+1}^3 is divided into m identical segments. The optimum segment quantity m is known according to Lemma 1.

Step 4: Sensor node N_i should assist in delivering the mobicast message if $F_{t+1}(N_i) \leq 0$. $F_{t+1}(N_i) \leq 0$ implies N_i is located within ZOF_{t+1}^3. If sensor node N_i is located in a segment S_i with the highest priority, N_i waits the shortest defer time. Sensor node N_i firstly broadcast P_m when the defer time is zero.

Step 5: The size of a segment can adaptively adjust since the initial size of ZOF_{t+1}^3 may not accurately predict. To get a higher successful delivery rate with the largest node efficiency, the required minimum node quantity is n_m according to Lemma 2. That implies that the the mobicast control packet P_m should be delivered $n_m - 1$ hops to acquire a higher successful delivery rate. Let h_i denote as the number of hop of P_m delivery in sensor node N_i. Therefore, Sensor node N_i encounters the hole problem and is not able to deliver P_m, N_i can expand its segment with a range r to involve more sensor node to deliver P_m if $h_i \leq n_m - 1$. This is, the equatorial radius in this segment expands to $a + r$. Otherwise, N_i drops P_m. Therefore, each segment can dynamically expand based on the real size of a hole.

Step 1 creates various sizes of ZOF_{t+1}^3 to cover the hole based on the network density and the velocity of current flow in ZOR_t^3 as shown in Fig. 15. Observe that it may not accurately predict the size ZOF_{t+1}^3 by the network density nd_t and the velocity of current flows $\overrightarrow{C}$ in ZOR_t^3; therefore, Step 5 can real-time adjust the size of ZOF_{t+1}^3 based on the network density nd_{t+1} and the velocity of ocean current within ZOF_{t+1}^3.

Fig. 14 shows that a ZOF_{t+1}^3 is created by $F_{t+1}(N_i)$. Fig. 16 shows that the message delivery is obstructed by a hole. Sensor nodes N_2 cannot further deliver the mobicast message. Then the segment expands to a larger size since $h_2 \leq n_m - 1$. Sensor node N_6 terminates the P_m delivery because $h_6 \leq n_m - 1$.

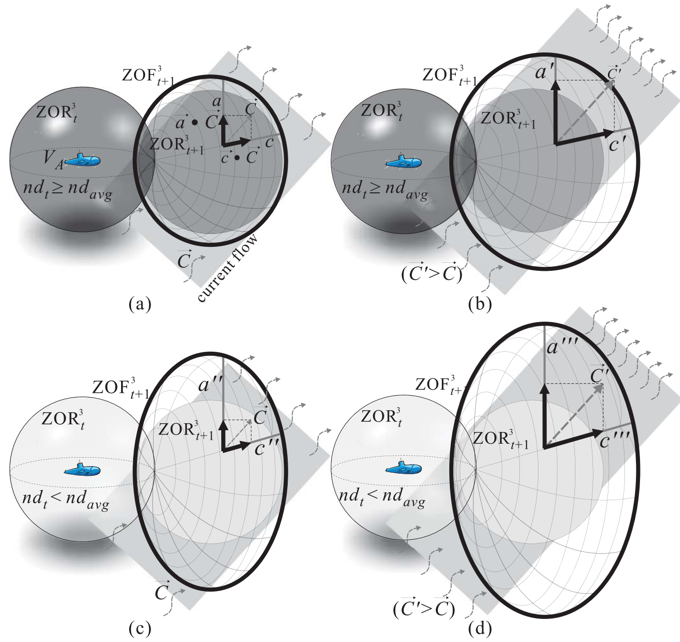

Fig. 15. Various size of ZOF_{t+1}^3 based on different network density and current flows (a) high density and the slow current, (b) high density and the fast current, (c) low density and the slow current, and (d) the high density and the fast current.

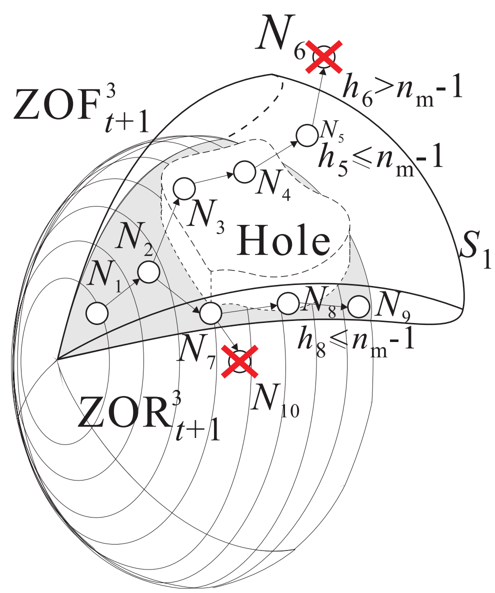

Fig. 16. Segment expands according to the hole.

C. 3-D ZOR_{t+1} Collection Phase

After all sensor nodes within ZOR_{t+1}^3 were waked up, the AUV can collect the sensed data from all sensor nodes within ZOR_{t+1}^3 at time $t+1$. The detailed operation is developed as follows.

Step 1: The AUV broadcasts the mobicast control packet $P_m(N_i, Z_{t+1}(N_i), m, r, \overrightarrow{v_A})$, where P_m is the control packet to control the delivery of mobicast message,

N_i is the ID of current sensor node, $Z_{t+1}(N_i)$ describes the region of ZOR^3_{t+1}, m is the mobicast message, r is the radius of hold and forward zone, and $\overrightarrow{v_A}$ is velocity vector of AUV.

Step 2: A sensor node N_i should send the sensed data to the AUV if $Z_{t+1}(N_i) \le 0$ when a sensor N_i receives a P_m. $Z_{t+1}(N_i) \le 0$ implies sensor node N_i is located within ZOR^3_{t+1}. Otherwise, if $Z_{t+1}(N_i) > 0$, sensor node N_i drops P_m.

Step 3: After the AUV left ZOR^3_{t+1}, all sensor nodes within ZOF^3_{t+1} switch to sleep mode for power saving.

V. Performance Analysis

This section provides theoretically proven bounds for the optimum segment quantity, the minimum node quantity, and the required segment quantity. The simulation results are then analyzed.

A. Performance Analysis

All sensor nodes are assumed in the analysis to be randomly deployed in the network. We have the following results.

Theorem 1: Given the successful communication probability p; then we know the low bound of successful delivery rate for delivering with L_R segments and all segments are $p^{\frac{L_L}{r}} \times \frac{\overrightarrow{s_i^o} \cdot \overrightarrow{C}}{r} \times L_R$ and $p^{\frac{L_L}{r}} \times \frac{2\pi a}{r}$ respectively, where L_L is the length of a segment and $L_L = \int_{-c}^{c} \sqrt{1 + \frac{(a-c)(a+c)z^2}{c^4}} dz$.

Proof: The mobicast message should deliver via sensor nodes in ZOF^3_{t+1} when the delivery in ZOR^3_{t+1} encounters a hole problem. We assume a worse case which sensor nodes only exist on the surface of ZOF^3_{t+1}. Since ZOF^3_{t+1} is split into $m = \frac{2\pi a}{\overrightarrow{s_i^o} \cdot \overrightarrow{C}}$ segments, we should compute the successful delivery rate in a segment. A segment can exist $\frac{\overrightarrow{s_i^o} \cdot \overrightarrow{C}}{r}$ routing paths to deliver the mobicast message because the width of a segment is $\overrightarrow{s_i^o} \cdot \overrightarrow{C}$. Each routing path has $\frac{L_L}{r}$ hops to deliver since the length of a segment $L_L = \int_{-c}^{c} \sqrt{1 + \frac{(a-c)(a+c)z^2}{c^4}} dz$. So we can use $p^{\frac{L_L}{r}} \times \frac{\overrightarrow{s_i^o} \cdot \overrightarrow{C}}{r}$ to describe the successful delivery rate in a segment. Therefore, the successful delivery rate is $p^{\frac{L_L}{r}} \times \frac{\overrightarrow{s_i^o} \cdot \overrightarrow{C}}{r} \times L_R$ when L_R segments are used to deliver the mobicast message. When all segments $m = \frac{2\pi a}{\overrightarrow{s_i^o} \cdot \overrightarrow{C}}$ are used to deliver, the successful delivery rate is $p^{\frac{L_L}{r}} \times \frac{\overrightarrow{s_i^o} \cdot \overrightarrow{C}}{r} \times \frac{2\pi a}{\overrightarrow{s_i^o} \cdot \overrightarrow{C}} = p^{\frac{L_L}{r}} \times \frac{2\pi a}{r}$. ■

Theorem 2: Given a ZOF^3_{t+1}; then the upper bound of message overhead for delivering with L_R segments and all segments are $\frac{(m-L_R)}{m} + L_R \times \frac{a^2 c}{m \times R^3}$ and $\frac{a^2 c}{R^3}$.

Proof: As shown in Fig. 17, the volume of a ZOR^3_{t+1} is $\frac{4}{3}\pi R^3$; therefore, the minimum transmitting times for delivering the mobicast message is $\frac{\frac{4}{3}\pi R^3}{r^3}$. The volume of a ZOR^3_{t+1} and 3-D ZOF^3_{t+1} is $(m - L_R) \times \frac{\frac{4}{3}\pi R^3}{m} + L_R \times \frac{\frac{4}{3}\pi a^2 c}{m}$ when L_R segments are used; so the transmitting times for

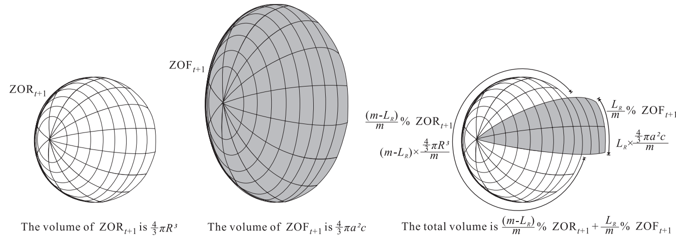

Fig. 17. Total volume of ZOR_{t+1} and L_R segments.

delivering the mobicast message is $\frac{(m-L_R) \times \frac{\frac{4}{3}\pi R^3}{m} + L_R \times \frac{\frac{4}{3}\pi a^2 c}{m}}{r^3}$. Therefore, when L_R segments are used to deliver the mobicast message, the multiple of message overhead is $\frac{(m-L_R) \times \frac{\frac{4}{3}\pi R^3}{m} + L_R \times \frac{\frac{4}{3}\pi a^2 c}{m}}{r^3} / \frac{\frac{4}{3}\pi R^3}{r^3} = \frac{(m-L_R)}{m} + L_R \times \frac{a^2 c}{m \times R^3}$. When all segments m (let $L_R = m$) are used to deliver the mobicast message, the multiple of message overhead is $\frac{a^2 c}{R^3}$. ■

Theorem 3: Given a ZOF^3_{t+1}; then the upper bound of power consumption for delivering with L_R segments and all segments are $\frac{(m-L_R) \times \frac{\frac{4}{3}\pi R^3}{m} + L_R \times \frac{\frac{4}{3}\pi a^2 c}{m}}{r^3} \times P_{tx} + (((m - L_R) \times \frac{\frac{4}{3}\pi R^3}{m} + L_R \times \frac{\frac{4}{3}\pi a^2 c}{m}) \times nd_t) \times P_{rx} + P_{sleep}$ and $\frac{\frac{4}{3}\pi a^2 c}{r^3} \times P_{tx} + (\frac{4}{3}\pi a^2 c \times nd_t) \times P_{rx} + P_{sleep}$ respectively, where P_{tx}, P_{rx}, and P_{sleep} are the power consumption for transmitting, receiving, and sleeping respectively.

Proof: Since the transmitting times for delivering the mobicast message is $\frac{(m-L_R) \times \frac{\frac{4}{3}\pi R^3}{m} + L_R \times \frac{\frac{4}{3}\pi a^2 c}{m}}{r^3}$ when L_R segments are used, the total transmission power is $\frac{(m-L_R) \times \frac{\frac{4}{3}\pi R^3}{m} + L_R \times \frac{\frac{4}{3}\pi a^2 c}{m}}{r^3} \times P_{tx}$. The volume of a ZOR^3_{t+1} and ZOF^3_{t+1} is $(m - L_R) \times \frac{\frac{4}{3}\pi R^3}{m} + L_R \times \frac{\frac{4}{3}\pi a^2 c}{m}$ when L_R segments are used; therefore, there exists $((m - L_R) \times \frac{\frac{4}{3}\pi R^3}{m} + L_R \times \frac{\frac{4}{3}\pi a^2 c}{m}) \times nd_t$ nodes. A total $((m - L_R) \times \frac{\frac{4}{3}\pi R^3}{m} + L_R \times \frac{\frac{4}{3}\pi a^2 c}{m}) \times nd_t$ nodes are necessary to receive the mobicast message. The total receiving power is$(((m-L_R) \times \frac{\frac{4}{3}\pi R^3}{m} + L_R \times \frac{\frac{4}{3}\pi a^2 c}{m}) \times nd_t) \times P_{rx}$. Therefore, the total power consumption is $\frac{(m-L_R) \times \frac{\frac{4}{3}\pi R^3}{m} + L_R \times \frac{\frac{4}{3}\pi a^2 c}{m}}{r^3} \times P_{tx} + (((m - L_R) \times \frac{\frac{4}{3}\pi R^3}{m} + L_R \times \frac{\frac{4}{3}\pi a^2 c}{m}) \times nd_t) \times P_{rx}$. ■

B. Simulation Results

Our paper presents a mobicast routing protocol in underwater sensor networks. The protocols are mainly implemented using the ns2 simulator and Aqua-Sim emulator [13]. Our mobicast routing protocol is simulated compared to a direct delivery without ZOF^3_{t+1}, the proposed scheme, and RMTG [8], which are denoted as MUW, Proposed Protocol, and RMTG, respectively. The simulation environment is shown as Fig. 18. In the simulation, all underwater sensor nodes are randomly distributed in a 3-D underwater environment in the sea to form a 3-D USN. Therefore, some regions may deploy more sensor nodes and the other regions may deploy fewer sensor nodes. When the simulation is starting,

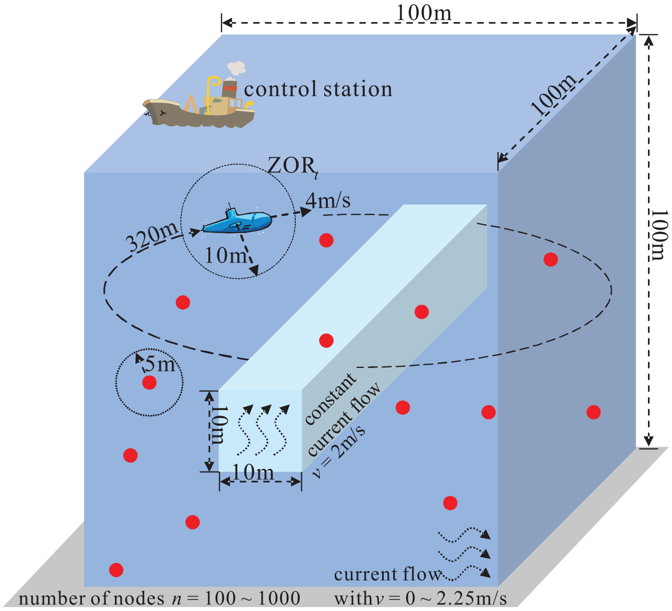

Fig. 18. Simulation environment and parameters.

sensor nodes are drifted away due to the ocean current and a hole may appear. The system parameters are given below. To discuss the effect of the network density (ND) of a USN, our simulator considers a 3-D cubic region with a size of $100 \times 100 \times 100$ units with various numbers of nodes, ranging from 100 to 1000. The communication range of a sensor node and the AUV are 5 units and 10 units, respectively. The radius of ZOR$_t$ is 10 m. The velocity of AUV is constant 4 m/sec. The velocity of current flow (v) is from 0 to 2.25 m/sec. The time interval between time t and $t+1$ is 5 seconds. We set the power consumption parameters based on the underwater acoustic modem, UMW1000, from LinkQuest [14]. The power consumption on transmission mode, receive mode, and sleep mode are 2 Watts, 0.75 Watts, and 8 mW, respectively. It is noted that Proposed Protocol-A and MUW-A are denoted as the analyzed results of Proposed Protocol and MUW, respectively, which derived from the performance analysis in Section V-A, respectively. The performance metrics to be observed are:

1) The *successful delivery rate* (SDR) is the number of nodes located in ZOR$^3_{t+1}$ which can successfully receive the mobicast messages and wake up, divided by the total number of nodes in ZOR$^3_{t+1}$.
2) The *power consumption* (PC) is the total power consumption that all sensor nodes consumed.
3) The *message overhead* (MO) is the total number of packets that all sensor nodes transmitted, including the control and mobicast messages, divided by the minimum number of packets used in our mobicast protocol.
4) The *average delay time* (DT) is the total delivery delay time divided by the total number of nodes in ZOR$^3_{t+1}$.
5) The *throughput* (TP) is the total number of data packets which the AUV receives from sensor nodes in ZOR^3_t per second.

It is worth mentioning that an efficient mobicast protocol in a USN is achieved with a high SDR, low PC, and low MO.

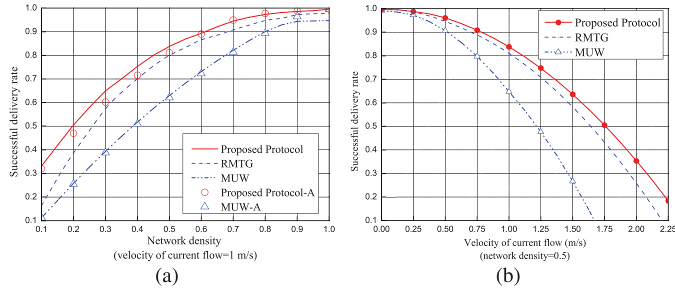

Fig. 19. Performance of successful delivery rate versus (a) network density and (b) current velocity.

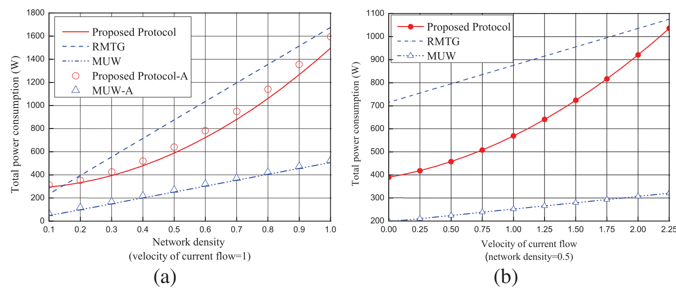

Fig. 20. Performance of power consumption versus (a) network density and (b) current velocity.

In the following, we illustrate our simulation results for *successful delivery rate* (SDR), *power consumption* (PC), and *message overhead* (MO) from several aspects.

1) Successful Delivery Rate (SDR): The simulation results of the SDR under various network density (ND) and velocity of current flow (v) are shown in Fig. 19. We observed that the SDR of Proposed Protocol, MUW, and RMTG were high as the network density was high. Proposed Protocol and MUW were nearly equal to Proposed Protocol-A and MUW-A respectively, as illustrated in Fig. 19(a). Fig. 19(a) shows the observed SDR under various NDs. A mobicast protocol with the high successful delivery rate implies that the value of its SDR was high. The higher the ND is, the higher the SDR will be. It was observed that SDR was very low when ND < 0.2 because several sensor nodes were totally isolated under very low density. The SDR of RMTG is closed to Proposed Protocol when ND > 0.8. This is because the delivery rate is high under high network density. The SDR of MUW is lower under the low network density because sensor nodes are not enough to deliver messages. Fig. 19(b) shows the observed SDR under various v. The higher the v is, the lower the SDR will be. This is because sensor nodes are drifted by the current flow. Lots of sensor nodes are drifted out of ZOF$^3_{t+1}$ when the velocity of current flow is high; therefore, the mobicast message is difficult to successfully deliver when the velocity of current flow is high and then the SDR drops. The SDR of MUW drops quickly when the v is higher because sensor nodes are not sufficient to deliver the mobicast message under a higher v.

2) Power Consumption (PC): The simulation results of the PC under various network density (ND) and velocity of current flow (v) are shown in Fig. 20. We observed that the PC of Proposed Protocol, MUW, and RMTG were high as the network density was high. Proposed Protocol and MUW were

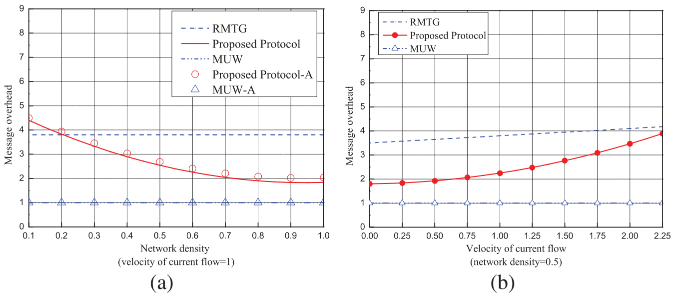

Fig. 21. Performance of message overhead versus (a) network density and (b) current velocity.

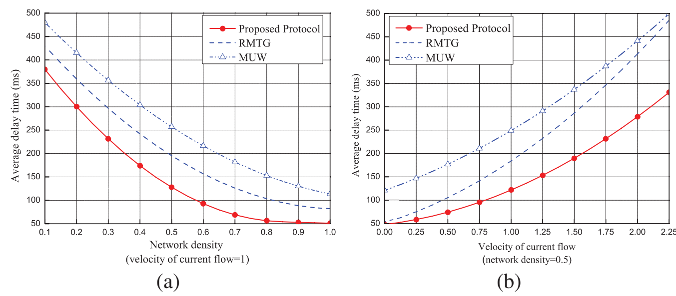

Fig. 22. Performance of average delay time versus (a) network density and (b) current velocity.

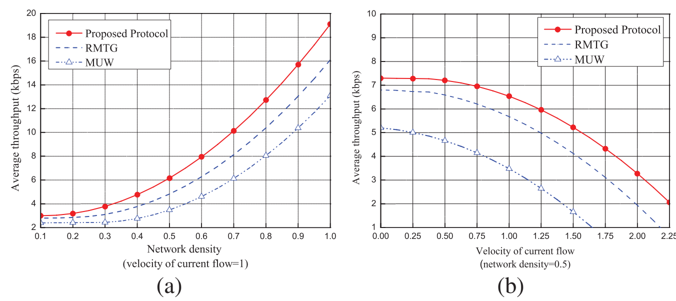

Fig. 23. Performance of average throughput versus (a) network density and (b) current velocity.

nearly equal to Proposed Protocol-A and MUW-A respectively, as illustrated in Fig. 20(a). Fig. 20(a) shows the observed PC under various NDs. A mobicast protocol with the low power consumption implies that the value of its PC was low. The higher the ND is, the higher the PC will be. This is because more and more nodes are involved to deliver messages. Fig. 20(b) shows the observed PC under various υ. The higher the υ is, the higher the PC will be. This is because that the size of 3-D ZOF_{t+1} is larger when the velocity of current flow υ is higher. The curve of the PC of Proposed Protocol is lower than that of RMTG under various velocity of current flow υ. The PC of Proposed Protocol segments increases quickly when the velocity of current flow υ is higher. This is because the size of each segment is large when υ is high; therefore, more sensor nodes are involved to deliver messages and consume much power.

3) Message Overhead (MO): The simulation results of the MO under various network density (ND) and velocity of current flow (υ) are shown in Fig. 21. We observed that the MO of Proposed Protocol was low as the network density was high. Proposed Protocol and MUW were nearly equal to Proposed Protocol-A and MUW-A respectively, as illustrated in Fig. 21(a). Fig. 21(a) shows the observed MO under various NDs. A mobicast protocol with the low message overhead implies that the value of its MO was low. The higher the ND is, the lower the MO will be. This is because more and more nodes are involved to deliver messages. Fig. 21(b) shows the observed MO under various υ. The higher the υ is, the higher the MO will be. This is because that the size of 3-D ZOF_{t+1} is larger when the velocity of current flow υ is higher. The curve of the MO of Proposed Protocol is lower than that of RMTG under various velocity of current flow υ. The MO of Proposed Protocol segments increases quickly when the velocity of current flow υ is higher. This is because the size of each segment is large when υ is high; therefore, more sensor nodes are involved to deliver messages and a lots of message are generated.

4) Average Delay Time (DT): The simulation results of the DT under various network density (ND) and velocity of current flow (υ) are shown in Fig. 22. We observed that the DT of MUW, Proposed Protocol, RMTG were low as the network density was high. Fig. 22(a) shows the observed DT under various NDs. A mobicast protocol with the low delivery delay time implies that the value of its DT was low. The higher the ND is, the lower the DT will be. This is because more and more nodes are involved to deliver messages. The curve of the DT of Proposed Protocol is lower than that of RMTG under various current flow υ. This is because that our scheme can dynamically and independently expand each segment; therefore, the shape of ZOF^3_{t+1} can fit the hole and deliver the message. The greater part of sensor nodes can successfully receive the message. RMTG always expands a constant size of forwarding zone, the hole problem may not be overcame. Many sensor nodes do not receive the message. The average delay time increases since a lot of sensor nodes wait a long time until the message time out.

Fig. 22(b) shows the observed DT under various υ. The higher the υ is, the higher the DT will be. This is because that a part of sensor nodes may be drifted by the ocean currents and the message should be re-transmitted and the delay time is increased. The curve of the DT of Proposed Protocol is lower than that of RMTG under various velocity of current flow υ. This is because the segment can dynamically expand to tolerate the increasingly current flow. The DT of RMTG increases quickly when the velocity of current flow υ is higher. This is because the constant size of forwarding zone is difficult to tolerate the increasingly current flow.

5) Throughput (TP): The simulation results of the TP under various network density (ND) and velocity of current flow (υ) are shown in Fig. 23. We observed that the TP of MUW, Proposed Protocol, and RMTG were high as the network density was high. Fig. 23(a) shows the observed TP under various NDs. A mobicast protocol with the high throughput implies that the value of its TP was high. The higher the ND is, the higher the TP will be. It was observed that TP was very low when ND < 0.2 because several sensor nodes were totally isolated under very low density. The curve of the DT of Proposed Protocol is higher than that of RMTG under various NDs. This is because that Proposed Protocol successfully wakes up more sensor nodes in ZOR^3_{t+1} than RMTG; therefore, the AUV with Proposed Protocol can receive more data than with RMTG. The TP of Proposed Protocol is lower under the low network density because fewer sensor nodes deliver data to the AUV.

Fig. 23(b) shows the observed TP under various υ. The higher the υ is, the lower the TP will be. This is because sensor nodes are drifted by the current flow. Lots of sensor nodes are drifted out of ZOF^3_{t+1} when the velocity of current flow is high; therefore, fewer sensor nodes wake up to deliver data to the AUV and the TP drops. The TP of Proposed Protocol drops quickly when the υ is higher because more sensor nodes are failed to wake up for data delivery under a higher υ.

VI. Conclusion

In this paper, we present a mobicast routing protocol to dynamically estimate the accurate 3-D ZOF_{t+1} to successfully deliver mobicast messages to wake up all sensor nodes in 3-D ZOR_{t+1} and overcome the hole problem and the ocean current effect by expanding the adaptive segments. Finally, the simulation results illustrated our performance achievements in terms of successful delivery rate, power consumption, and message overhead.

References

[1] J. Heidemann, Y. Li, A. Syed, J. Wills, and W. Ye, "Underwater sensor networking: Research challenges and potential applications," USC/ISI, Marina del Rey, Tech. Rep. ISI-TR-2005-603, 2005.

[2] I. F. Akyildiz, D. Pompili, and T. Melodia, "State-of-the-art in protocol research for underwater acoustic sensor networks," in *Proc. ACM Int. Workshop Underwater Netw.*, 2006, pp. 7–16.

[3] N. C. Nicolaou, A. G. See, P. Xie, J. H. Cui, and D. Maggiorini, "Improving the robustness of location-based routing for underwater sensor networks," in *Proc. IEEE Oceans*, Aberdeen, Scotland, Jun. 2007, pp. 1–6.

[4] D. Walker, "Micro autonomous underwater vehicle concept for distributed data collection," in *Proc. IEEE Oceans*, Boston, MA, Sep. 2006, pp. 1–4.

[5] Y. S. Chen, Y. W. Lin, Y. J. Liao, and G. M. Chiu, "HVE-mobicast: A hierarchical-variant-egg-based mobicast routing protocol for sensornets," *Telecommun. Syst.*, vol. 41, no. 2, pp. 121–140, 2009.

[6] Y. S. Chen, S. Y. Ann, and Y. W. Lin, "VE-mobicast: A variant-egg-based mobicast routing protocol for sensornet," *ACM Wireless Netw.*, vol. 14, no. 2, pp. 199–218, 2008.

[7] S. Park, B. Jo, and D. S. Han, "An efficient MAC protocol for data collection in underwater wireless sensor networks," in *Proc. IEEE Military Commun. Conf.*, Boston, MA, Jan. 2009, pp. 1–5.

[8] S. K. Dhurandher, M. S. Obaidat, and M. Gupta, "A novel geocast technique with hole detection in underwater sensor networks," in *Proc. ACS/IEEE Int. Conf. Comput. Syst. Appl.*, Hammamet, Tunisia, May 2010, pp. 1–8.

[9] J. Wang, D. Li, M. Zhou, and D. Ghosal, "Data collection with multiple mobile actors in underwater sensor networks," in *Proc. Int. Conf. Distrib. Comput. Syst. Workshops*, Beijing, China, Jun. 2008, pp. 216–221.

[10] W. K. G. Seah, H. X. Tan, Z. Liu, and M. H. Ang, "Multiple-UUV approach for enhancing connectivity in underwater ad-hoc sensor networks," in *Proc. IEEE Oceans*, Washington, DC, Sep. 2005, pp. 2263–2268.

[11] A. Y. Teymorian, W. Cheng, L. Ma, X. Cheng, X. Lu, and Z. Lu, "3D underwater sensor network localization," *IEEE Trans. Mobile Comput.*, vol. 8, no. 12, pp. 1610–1621, Dec. 2009.

[12] S. Amari and H. Nagaoka, *Methods of Information Geometry*. New York: Oxford Univ. Press, 2000.

[13] P. Xie, Z. Zhou, Z. Peng, H. Yan, T. Hu, J.-H. Cui, Z. Shi, Y. Fei, and S. Zhou, "Aqua-sim: An NS-2 based simulator for underwater sensor networks," in *Proc. MITS/IEEE OCEANS*, Biloxi, MS, Oct. 2009, pp. 26–29.

[14] *LinkQuest*. (2011) [Online]. Available: http://www.link-quest.com/

Yuh-Shyan Chen received the B.S. degree in computer science from Tamkang University, Taipei, Taiwan, in June 1988, and the M.S. and Ph.D. degrees in computer science and information engineering from National Central University, Jhongli, Taiwan, in 1991 and 1996, respectively.

He has been a Professor with the Department of Computer Science and Information Engineering, National Taipei University, Taipei, since 2006. Since 2012, he is serving as Chairperson of the Department of Computer Science and Information Engineering, National Taipei University. His current research interests include wireless communications, mobile computing, and next-generation personal communication system.

Dr. Chen received the 2001 IEEE 15th ICOIN-15 Best Paper Award. He was a recipient of the 2005 Young Scholar Research Award, National Chung Cheng University. He served as the Editor-in-Chief of the *International Journal of Ad Hoc and Ubiquitous Computing* (indexed by SCIE and EI), the Regional Editor (Asia and Pacific) of *IET Communications*, the Editorial Board of *Telecommunication System Journal*, the *EURASIP Journal on Wireless Communications and Networking*, the *International Journal of Communication Systems, Mobile Information Systems*, the *Journal of Internet Technology*, and the *IET Networks*. He is a senior member of the IEEE Communication Society.

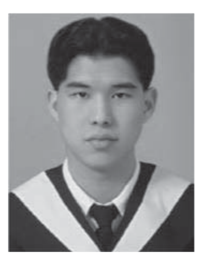

Yun-Wei Lin received the B.S. degree in computer and information science from Aletheia University, Taipei, Taiwan, in June 2003, and the M.S. and Ph.D. degrees in computer science and information engineering from National Chung Cheng University, Chiayi, Taiwan, in 2005 and 2011, respectively.

His current research interests include mobile ad hoc network, wireless sensor network, underwater sensor networks, vehicular ad hoc networks, green computing, and information-centric networking.